Journal of Molecular Structure 1247 (2022) 131343

Contents lists available at ScienceDirect

Journal of Molecular Structure

journal homepage: www.elsevier.com/locate/molstr

Synthesis of 7-azaindole based carbohydrazides and 1,3,4-oxadiazoles; Antioxidant activity, α-glucosidase inhibition properties and docking study

Samet Izgi[a], Ibrahim F. Sengul[b], Engin Şahin[c], Mehmet Serdar Koca[d], Fatma Cebeci[c,*], Hakan Kandemir[a,*]

[a] Department of Chemistry, Faculty of Art and Science, Tekirdag Namık Kemal University, Turkey
[b] Department of Chemistry, Faculty of Science, Gebze Technical University, Gebze, Kocaeli, Turkey
[c] Department of Nutrition and Dietetics, Faculty of Health Sciences, Bayburt University, Bayburt, Turkey
[d] Deparment of Molecular Biology and Genetics, Faculty of Science, Gebze Technical University, Gebze, Kocaeli, Turkey

ARTICLE INFO

Article history:
Received 28 July 2021
Revised 14 August 2021
Accepted 18 August 2021
Available online 24 August 2021

Keywords:
7-azaindole
1,3,4-oxadiazole
α-glucosidase inhibition
Antioxidant activity
Docking study

ABSTRACT

In this current work, 7-azaindole based 1,3,4-oxadiazoles have been successfully prepared by treatment of 3-(hydrazonomethyl)-7-azaindole with the different acyl chlorides or acetic anhydrides to give the corresponding carbohydrazides, followed by iodine mediated synthetic protocol in order to afford the corresponding 2,5-disubstituted 1,3,4-oxadiazoles. The full characterization data of the novel compounds were obtained by utilizing ^{1}H NMR, ^{13}C NMR, FT-IR, high-resolution mass spectrometry and single crystal X-ray diffraction techniques. The antioxidant activity and α-glucosidase inhibition potential of the prepared compounds are examined by *in vitro* assays. The targeted hydrazide linked 7-azaindoles and their corresponding cyclized form 1,3,4-oxadiazoles exhibited inhibitory potential with IC_{50} values ranges between 0.46 and 24.92 mM. Plausible binding mode and interaction of ligands with α-glucosidase enzyme have been studied by molecular docking, supporting the experimental results.

1. Introduction

The design and synthesis of nitrogen containing heterocyclic compounds for biological studies is an active area of research especially in the fields of organic and medicinal chemistry [1–4]. Among the various nitrogen containing heterocycles, indole moieties have been attractive targets within drug discovery due to the fact that naturally occurring indoles often display diverse and interesting biological activities [5–9]. Being a good bioisostere of naturally occurring indole alkaloids, azaindoles are a class of heterocycles consisting of a fused electron-deficient pyridine ring with electron-rich pyrrole ring [10]. It is well established that there are four different structural isomers of azaindoles which are known as 4-, 5-, 6- and 7-azaindoles resulting from the position of the nitrogen atom within the pyridine ring [11,12]. Of these isomers, the 7-azaindole is undoubtedly one of the more common and popular frameworks [13,14]. Structures containing 7-azaindole units have been the target of extensive studies due to their remarkable biological activities [14–16]. For example, 7-azaindole derivative natural product the variolin B, isolated from Antarctic sponge, has been used as an antiviral agent. Additionally, the 7-azaindole based 1,3,4-oxadiazoles showed promising CDC7 cell activity and selectivity profiles against CDK1, CDK2 and CDK9 inhibitors [17,18].

Apart from biological properties, 7-azaindole based molecules have been shown to possess a range of application including chemical sensor, field-effect transistors, organic light-emitting diodes (OLEDs) [19–21]. From the synthetic point of view, the most reactive position on 7-azaindole with respect to electrophilic aromatic substitution reaction is C3 [22]. The active sides of 7-azaindole ring system provides an opportunity for functionalization and derivatization. Consequently, design and synthesis of novel 7-azaindole based platforms is still desirable in both synthetic organic and medicinal chemistry.

On the other hand, the 1,3,4-oxadiazoles are unique heterocyclic systems and rapid development in the chemistry of 1,3,4-oxadiazole has been observed in the last few decades due to their important biological properties [23,24]. These five-membered nitrogen containing heterocycles play a vital role especially in medicinal chemistry [23,24]. Among biologically active 1,3,4-oxadiazoles, 2,5-disubstituted derivatives have gained special attention due to a wide range of pharmacological activities namely, antiviral, antibacterial, anti-fungal, anti-inflammatory and antihypertensive

* Corresponding authors.
E-mail addresses: fatmacebeci@bayburt.edu.tr (F. Cebeci), hkandemir@nku.edu.tr (H. Kandemir).

https://doi.org/10.1016/j.molstruc.2021.131343
0022-2860/

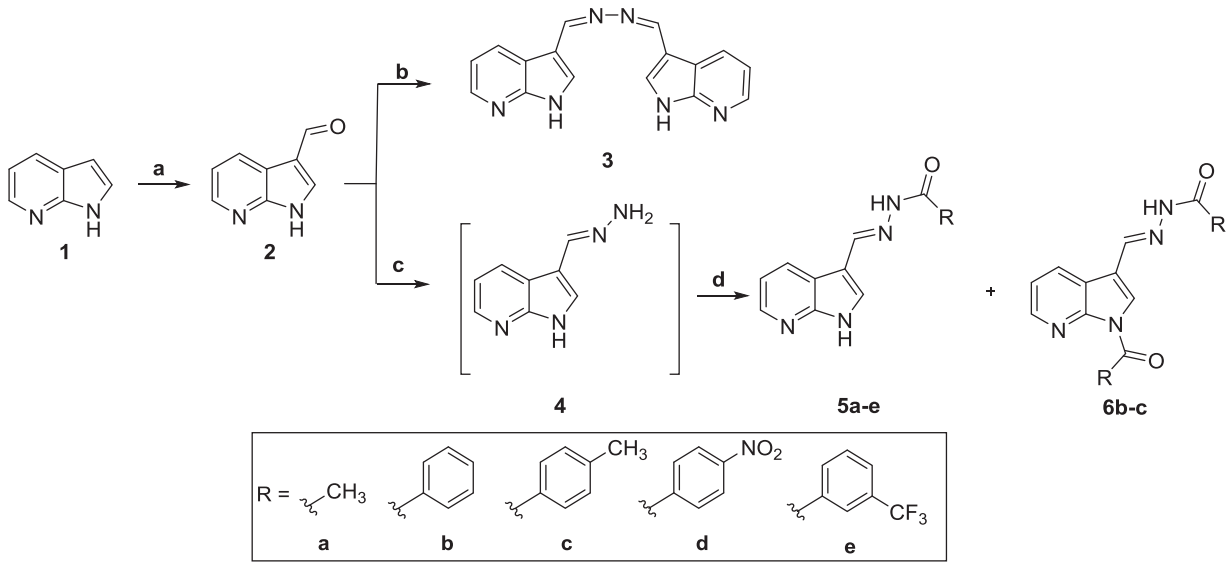

Scheme 1. Reagents and Conditions: (a) HMTA, CH_3COOH, H_2O; (b) excess $NH_2NH_2.H_2O$, EtOH, reflux, 3 h; (c) excess $NH_2NH_2.H_2O$, THF, r.t., 24 h; (d) RCOCl or acetic anhydride, Et_3N CH_3CN, r.t.

[25–29]. Antioxidant and acetylcholinestrase inhibition properties of indole based 1,3,4-oxadiazoles have been recently reported by us [30]. Furthermore, 1,3,4-oxadiazole-containing compounds have been used as the α-glucosidase inhibitors [31]. The compounds containing –NH–NH–C=O– moiety are known as hydrazide linkers which are employed as key intermediate building blocks in the preparation of 2,5-substituted-1,3,4-oxadiazole compounds [32]. It is worth noting here that hydrazide linkers are also important targets due to their potential biological activities. For example, a series of hydrazide intermediates and their corresponding 1,3,4-oxadiazoles were developed with displaying the best DPPH scavenging activity [32].

Considering the importance of 7-azaindole and 1,3,4-oxadiazole nucleus and encouraged by our recently reported indole based 1,3,4-oxadiazoles study, it is worthwhile to design and synthesis a new skeleton of both 7-azaindole and 1,3,4-oxadiazole motifs, which was expected to possess good antioxidant activity along with α-glucosidase inhibitor potentials. Furthermore, molecular docking study was performed in order to obtain structural insight into the inhibitory mechanisms for the α-glucosidase inhibitors. This is the first report about the preparation of targeted systems and the designated biological properties.

2. Results and discussion

2.1. Synthesis and characterization

For this current study, 7-azaindole was selected as the parent pharmacophore since nitrogen containing heterocycles have been frequently used in the area of organic and medicinal chemistry. The targeted 7-azaindole based carbohydrazide intermediates and 1,3,4-oxadiazoles were synthesized following the sequential reactions mentioned in Schemes 1 and 2. Aldehyde is an important functional groups to introduce functionality to the organic molecules and the synthetic strategy began with formylation of 7-azaindole. For this purpose, 7-azaindole-3-carbaldehyde **2** was synthesized in high yield by the one pot reaction of the commercially available 7-azaindole **1** with hexamethylenetetramine in acetic acid according to reported procedure [22]. 7-Azaindole possesses the aldehyde group is particularly suited to Schiff base reactions by employing hydrazine hydrates. The synthesis of (3-(hydrazonomethyl)-7-azaindole **3** was subsequently examined since they could serve as key intermediate building blocks in the preparation of unsymmetrical hydrazide linkages. When excess amount of hydrazine hydrate was added to 7-azaindole-3-carbaldehyde **2** in ethanol at reflux for 1 h, unexpected dimeric 7-azaindole **3** was obtained. It was found from the literature that the dimeric compound **3** was previously reported with the lack of ^{13}C NMR and mass spectroscopy data [33]. The detailed ^{1}H NMR, ^{13}C NMR and mass spectra are given in SI. When the reaction conditions were slightly modified, the monomeric compound **4** was afforded as the only product. At the beginning, the reaction of carbaldehyde **2** with excess hydrazine hydrate was carried out at room temperature and the product was formed in 80% yield, however, seven days reaction time was non-objectionable. Therefore, different solvents such as CH_3CN, DMF and THF were used to shorten the reaction time. The reaction with CH_3CN lasted in 2 days with acceptable yield. The reaction was completed in DMF in a day but the yield was very poor. To this end, the reaction of 7-azaindole-3-carbaldehyde **2** with excess amount of hydrazine hydrate in THF at room temperature afforded the monomeric compound **4** in 80% yield. The next step was performed immediately due to the low stability of 7-azaindole **4**.

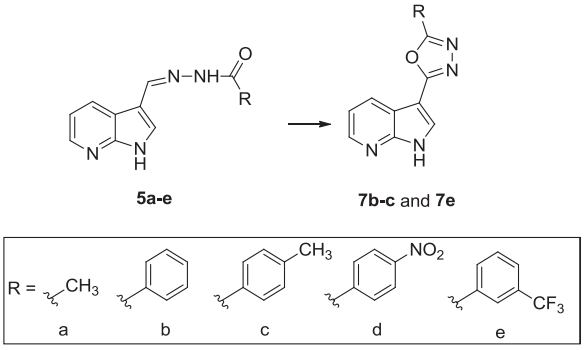

Scheme 2. Reagents and Conditions: DMSO, I_2, K_2CO_3, 110 °C, 24 h.

For the synthesis of unsymmetrically hydrazide bridged compounds, the compound **4** was reacted with acetic anhydride in acetonitrile in the presence of triethylamine, hydrazide linked 7-azaindole **5a** was generated as a single product in 95% yield. The compound **4** was subsequently reacted with *m*- and *p*-substituted

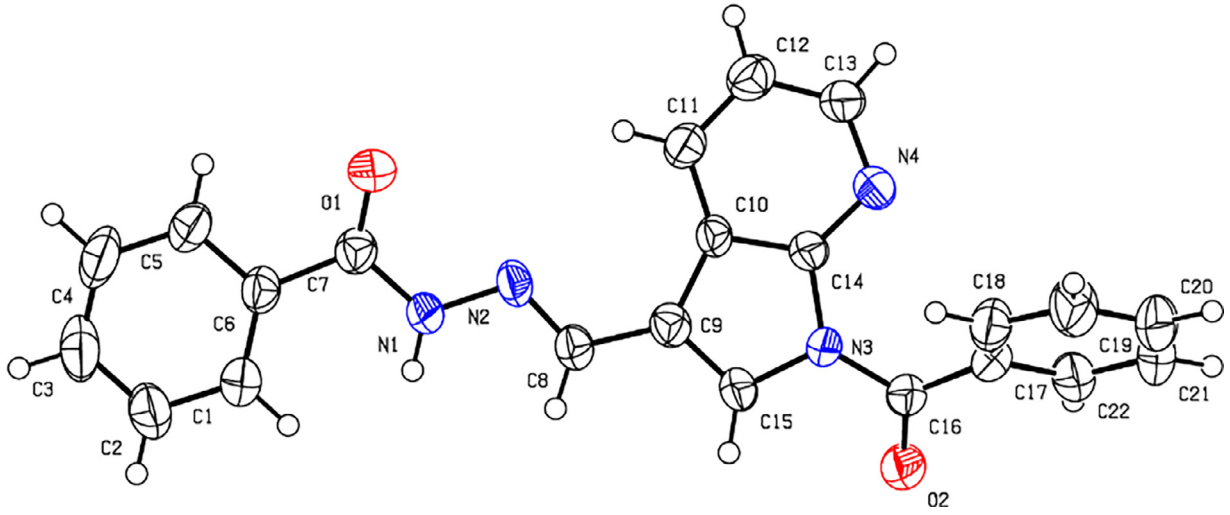

Fig. 1. The X-ray crystal structure of the compound **6b**.

benzoyl chloride derivatives under the same reaction conditions in order to produce the corresponding **5b–e**. It was revealed that the compounds **5d** and **5e** were obtained as single products. However, two products were obtained when the compound **4** was reacted with benzoyl chloride and tosyl chloride. The major products, obtained in 80% and 85% yields, were identified as the desired carbohydrazides **5b** and **5c**, while the minor products were identified as the di-reacted compound **6b** and **6c** in 21% and 19% yields. It was assumed that the presence of electron withdrawing groups such as NO_2 or CF_3 on the benzene ring may not allow to the formation of double attachments.

The ^{1}H NMR and ^{13}C NMR spectra of compound **5c** were characteristic for compounds **5a–e**. The ^{1}H NMR spectrum of the compound **5c** showed the characteristic amide NH peaks at 12.24 ppm as a singlet along with 7-azaindole NH resonated at 11.56 ppm. The ^{13}C NMR spectrum of the compound **5c** showed amide carbonyl peak at 162.9 ppm. Additionally, the molecular weight of the compounds **5a-e** were determined by high resolution mass spectrometry, which revealed the anticipated molecular ion peaks at 203, 265, 279, 309, 333 (M+1), respectively.

On the other hand, the ^{1}H NMR and ^{13}C NMR spectra of compound **6b** were characteristic for compounds **6b** and **6c**. The ^{1}H NMR spectrum of compound **6b** showed the presence of a singlet at 12.00 ppm corresponding to the amide proton. The disappearance of the 7-azaindole NH proton indicated that addition of benzoyl chloride to pyrrole ring of 7-azaindole had taken place. The ^{13}C NMR spectra showed two carbonyl peaks of the compound **6b** at 163.5 and 167.5 ppm. The structure of compound **6b** was further confirmed through X-ray crystallography which showed that both 7-azaindole NH and hydrazonomethyl NH had been substituted with the benzoyl chlorides (Fig. 1). The detailed structure and crystal parameters are present in Fig. S2 and Table S1.

Having these successful results in hand, the corresponding ring closure of 7-azaindole carbohydrazides **5a–e** into the corresponding 2,5-disubstituted-1,3,4-oxadiazoles was investigated. A variety of methods was therefore investigated for the synthesis of 7-azaindole based 1,3,4-oxadiazoles. The 7-azaindolecarbohydrazide **5b** was employed as a compound in order to investigate the optimize reaction conditions.

Application of any of the reaction conditions described in Table 1. The highest yield of the target product **7b** was achieved by refluxing **5b** in dimethyl sulfoxide in the presence of iodine and potassium carbonate for 24h. Similarly, the synthesis of **7c** and **7e** was achieved in 51 and 48 % yields, respectively, employing the same reaction conditions. However, application of any of the reaction conditions described in Table 1 to the 1,3,4-oxadiazoles **7a** and **7d** was not successful.

Table 1
Cyclization of 5b under various reaction conditions.

Conditions	Temp. (°C)	Time (h)	Yield (%)
DMSO/DIB	r.t.	72	*
DMSO/DIB	110	48	45
DCM/DIB	r.t.	48	*
$CHCl_3$/DIB	r.t.	72	*
DMF/I_2, K_2CO_3	110	48	18
DMSO/I_2, K_2CO_3	85	48	*
DMSO/I_2, K_2CO_3	110	24	51

* No reaction

The structures of compounds **7b,c** and **7e** were supported by ^{1}H NMR and ^{13}C NMR spectroscopic data. The ^{1}H NMR spectrum of the compound **7b** in DMSO, as a typical example of the 7-azaindole based 1,3,4-oxadiaozles, showed the disappearance of the amide NH and imine CH protons of the starting material at 12.66 and 8.52 ppm which clearly confirmed that the cyclization had taken place. The high resolution mass spectrum further confirmed that tandem cyclization had occurred by showing a molecular ion at 263 ($M + 1$).

2.2. Biological Study

Two widely used antioxidant activity measurement assays namely DPPH (2,2-diphenyl-1-picryl-hydrazylhydrate) and ABTS (2,2′-azino-bis(3-ethylbenzothiazoline-6-sulfonic acid) were used in the current study in order to investigate the antioxidant activity of the targeted compounds. Table 2 shows both the DPPH radical scavenging and cationic ABTS radical activities of the all newly synthesized compounds. Ascorbic acid was employed as a positive control and gave almost similar results in the both assays. According to the results, the methyl substituted compound **5a** was found to be the most potent compound with the IC_{50} value of 10.12 ± 2.13 mM among the tested compounds in DPPH assay. The rest of the compounds show no activity for DPPH radical scavenging assay. On the hand, the cationic radical scavenging activities of the targeted compounds and control ascorbic acid are illustrated in Table 2 with IC_{50} concentration values. It is noteworthy that the cationic radical scavenging activities of the synthesized compounds were found to be more potent than DPPH radical scavenging activity. In the case of **6c**, with two *p*-methylbenzoyl groups

Table 2
The *in vitro* antioxidant activity of the compounds by DPPH and ABTS assays.

Compounds	IC_{50} (mM)±SD	
	DPPH	ABTS
3	ND	ND
5a	10.12 ± 2.13	55.71 ± 9.83
5b	ND	47.14 ± 1.55
5c	ND	0.78 ± 0.26
5d	ND	ND
5e	ND	1.49±0.19
6b	ND	4.65 ± 0.62
6c	ND	0.39 ± 0.02
7b	ND	11.24 ± 0.99
7c	ND	16.21 ± 2.06
7e	ND	ND
A.A	0.08 ± 0.00	0.09 ± 0.01

ND; not detected, AA; ascorbic acid, SD; standard deviation.

attached to the 1,3,4-oxadiazole moiety, the highest inhibition was obtained with a IC_{50} value of 0.39 ± 0.02 mM. The compound **5c** possesses one p-methylbenzoyl group attached to hydrazide linker exhibited the second best scavenging activity with the value of 0.78 ± 0.26 mM. Apart from the compounds **5c** and **6c**, the compounds were found to be less effective for the cationic radical scavenging activity assay. IC_{50} results of the targeted compounds illustrated that novel derivatives **5c** and **6c** have good potential for antioxidant study. In this context, the compounds **5c** and its cyclized form **6c** having the highest activity are promising compounds and need further investigation. The compound **5d**, with nitrobenzene linked to 1,3,4-oxadiazole scaffold, has shown no inhibition activity when compare to the antioxidant capacities of **5a**–**5e**. This result is in accordance with the previous study reporting the weaker antioxidant activity of compounds with nitro substituent [34]. It was revealed that the antioxidant activities of the designated molecules was found to be competitive with standard ascorbic acid.

Acarbose is α-glucosidase inhibitor decreases intestinal absorption of carbohydrates. It has been used as a standard drug for supporting therapy in the management of type 2 diabetes. Existing α-glucosidase inhibitors are confirmed to be safe and effective but their side effects such as abdominal bloating, abdominal cramps and diarrhea give trouble to the users so it is essential to look for novel and effective α-glucosidase inhibitors [35,36]. Since carbohydrazide linkers and 1,3,4-oxadiazoles were reported as α-glucosidase inhibitors, it was of interest to investigate α-glucosidase inhibition potential of the targeted 7-azaindole based carbohydrazides and 1,3,4-oxadiazoles. All the numerical IC_{50} values obtained from the experimental studies are represented in Table 3. Acarbose was employed as a positive control in this current work. Targeted compounds demonstrated varying degrees of α-glucosidase inhibitory potential with IC_{50} values ranging between 0.40 ± 0.17 and 24.92 ± 8.86 mM (Table 3). It was revealed that compounds **3, 6b** and **7e** showed much greater activities when compared to the rest of the compounds tested. Compounds **5c** and **6c** showed good to moderate activity, while compounds **5a, 5b, 5d, 5e, 7b** and **7c** showed no significant α-glucosidase inhibitory activity (Table 3). More specifically, the compound comprising benzoylchloride group on 7-azaindole NH and carbohydrazide NH **6b** was found to be most potent inhibitor among the series with an IC_{50} value of 0.40 ± 0.17 mM. The activity of compound **7e** with an IC_{50} value of 0.46 ± 0.15 mM on GAA inhibition was similar to that of 6b and it is the second most promising inhibitor candidate among tested. Furthermore, dimeric 7-azaindole analog **3** was also demonstrated high α-glucosidase inhibitory activity with IC_{50} value of 0.65 mM.

2.3. Computational analysis

The crystal structure of GAA complexed with AC1 and AC2 shows two distinct inhibitor binding pockets (Fig. 2 also interaction of ligands given Fig. S2). Among these, the first pocket corresponds to the active site of the GAA enzyme. Therefore, we have performed docking studies targeting these two pockets. Since the x-ray 3D structure of GAA-AC1-AC2 is known, we carried out self-docking studies to establish a good docking protocol. Fig. 2 shows the top ranked poses of self-docking of AC1 and AC2 on GAA using two different software. Both algorithms almost perfectly reproduced the experimental displacement of ligands. The Glide docking scores showed that the binding affinity of GAA to AC1 and AC2 is very strong (-16.7 and -10.5 kcal/mol, respectively) whereas the scores of Vina were somewhat lower (Table 3). The Glide and AutoDock vina scores are relatively in agreement with experimental IC_{50} values.

In addition to self-docking studies of AC1 and AC2 to GAA, we also docked all the synthesized of compounds to the same binding regions. Summary of best poses are present in Table 3.In the first pocket (the active site of the enzyme), although the absolute values produced by AutoDock vina are better fit with the experimental values, both algorithms perfectly predict the experimental trend among the synthesized compounds. Experimentally suggested candidate of **6b** and **7e** have the greatest docking scores in both algorithms among tested. It should be noted that even though **6b** and **7e** are the greatest among synthesized ligands, they all still have lower scores than AC1. This has been also confirmed by the experiments.

Table 3
The α-glucosidase inhibitory potential and docking scores of the compounds.

Compounds	Experimental Results		Schrodinger Best Pose (kcal/mol)		AutoDock vina Best Pose (kcal/mol)	
	IC_{50}(mM)±SD	ΔG(kcal/mol)	First Pocket	Second Pocket	First Pocket	Second Pocket
3	0.65 ± 0.09	-8.7	-3.4	-3.3	-7.2	-7.6
5a	ND	ND	-3.4	-4.1	-6.2	-6.7
5b	ND	ND	-4.0	-3.8	-7.2	-8.0
5c	4.53 ± 0.62	-7.9	-3.2	-2.7	-7.4	-7.9
5d	ND	ND	-3.5	-3.7	-6.9	-8.3
5e	ND	ND	-2.8	-4.6	-7.9	-8.2
6b	**0.40 ± 0.17**	**-8.3**	**-4.9**	**-3.4**	**-8.6**	**-8.0**
6c	24.92 ± 8.86	-6.4	-3.0	-1.6	-8.2	-8.8
7b	ND	ND	-3.0	-3.5	-7.8	-7.5
7c	ND	ND	-2.9	-3.0	-7.5	-7.4
7e	**0.46 ± 0.15**	**-8.5**	**-4.0**	**-3.2**	**-8.7**	**-8.1**
Acarbose	$1.75 \pm 0.39 \times 10^{-3}$	-10.7	-16.7	NA	-6.5	NA
Acarbose-derived trisaccharide	NA	NA	NA	-10.5	NA	-7.5

ND; not detected, NA; not available, SD; standard deviation. ΔG values were calculated $\Delta G = -RT\ln(IC_{50})$ at 298 K.

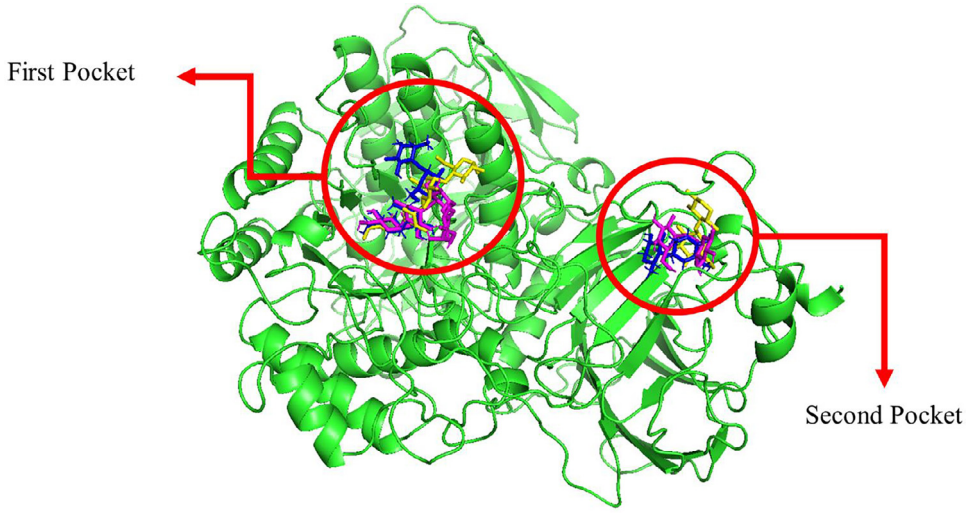

Fig. 2. Lysosomal alpha-glucosidase enzyme (GAA) complexed with alpha-acarbose (AC1, yellow sticks in the first pocket) and acorbose-derived trisaccharide (AC2, yellow sticks in the second pocket) inhibitors along with top ranked Glide (blue sticks) and AutoDock vina (purple sticks) poses.

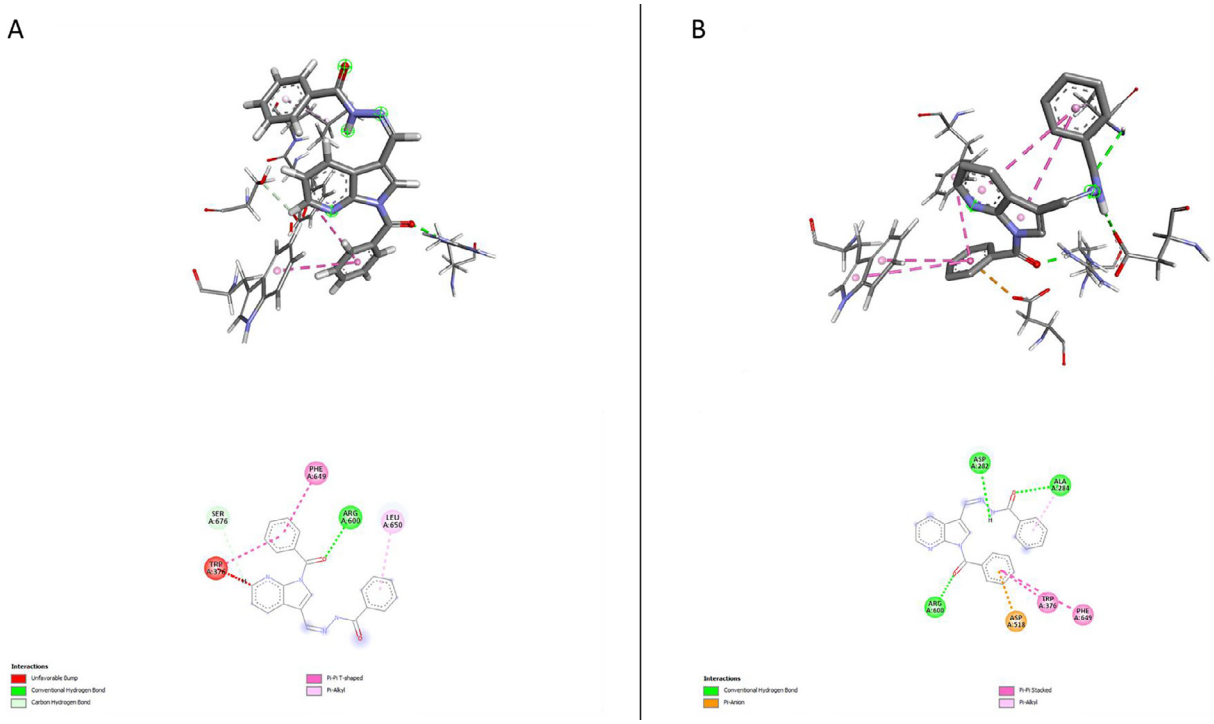

Fig. 3. Interaction map of top solution of 6b compound performed by (A) Glide and (B) AutoDock vina.

In accordance with AC1 and AC2, the top solutions of synthesized of compounds have almost identical positions for both Glide and AutoDock vina (comparison of top solutions for both programs are given on Fig. S3). Fig. 3 shows interaction map of top solution of 6b with GAA using Glide and AutoDock vina. Both programs predict the binding mode to be the same in which Arg600 makes strong hydrogen bonds with carbonyl oxygen of **6b**. Additionally, Trp376 and Phe649 make π-stacking interactions with phenyl ring of **6b** (interaction of 7e given Fig. S4).

It is also possible for these compounds to bind in the second pocket. Upon binding to the second pocket, they may or may not have allosteric inhibition mechanism. Our docking results suggest that **5b–e** and **6c** compounds have strong affinity to the second pocket. In particular, **6c** has the greatest affinity which was experimentally determined to show a moderate inhibition activity. This may indicate the compound is binding to the second pocket but having partial allosteric inhibition.

Overall docking analysis showed that AC1 affinity is the greatest in the first binding pocket (the active site of the enzyme). Among the synthesized compounds, **6b** and **7e** are the most promising candidates for GAA inhibition. Both Glide and AutoDock vina find very similar binding modes for AC1 and synthesized compounds in the first pocket. Some of the other compounds might be attaching from the second pocket, causing partial or no inhibition.

3. Conclusion

This study resulted in synthesis of novel 7-azindole based carbohydrazides and their corresponding oxadiazole derivatives which were tested for antioxidant activity and α-glucosidase inhibitory

potential. DPPH assay seemed to be not an applicable method to detect antioxidant activity for these compounds. Compound **6c** bearing two *p*-methylbenzoyl gruops attached to the 7-azaindole NH and carbohydrazide NH was found to be the best antioxidant compound for ABTS assay. The obtained data demonstrated that the 7azaindole-carbohydrazide intermediates could be promising structures than 7-azaindole-1,3,4-oxadiazole systems for the investigation of novel potent antioxidant scaffolds. In addition, 5 out of 11 compounds showed α-glucosidase inhibition activity. Docking studies are in relatively good agreement with experiments and showed **6b** and **7e** (among the synthesized) to have the greatest affinity for binding to GAA, which is still too low to compete with AC1. It was important to mention here that antioxidant and α-glucosidase inhibition studies on such 7-azaindole systems are not reported before.

4. Experimental section

4.1. Materials and methods

All reagents and solvents were obtained from commercial sources and appropriately purified, if necessary. The deuterated solvent (deutero dimethyl sulfoxide, $(CD_3)_2SO$, DMSO-d_6) for NMR spectroscopy was obtained from Merck. Measurements IR spectra were recorded between 4000 and 650 cm^{-1} using a Perkin Elmer Spectrum 100 FT-IR spectrometer. ^1H and ^{13}C NMR spectra were recorded in DMSO-d_6 solution at 298 K on a Varian 500 MHz spectrophotometer. Residual dimethyl sulfoxide ($(CH_3)_2SO$ in $(CD_3)_2SO$) and the central line of the deutero dimethyl sulfoxide (DMSO-d_5) quintet (δ = 2.50 ppm) was used for ^1H NMR spectra and the central line of the deutero dimethyl sulfoxide (DMSO-d_6) septet (δ = 39.5 ppm) was used for ^{13}C NMR spectra as an internal reference. Mass spectra reported to four decimal places were recorded on an Agilent 1260 Infinity Series 6230 LC/ TOF-MS.

*4.2. (1Z,2Z)-1,2-bis((1H-pyrrolo[2,3-b]pyridin-3-yl)methylene) hydrazine (**3**)*

Hydrazine hydrate (1 mL, 3 mmol) was added to a suspension of 7-azaindole-3-carbaldehyde (1.5 g, 1 mmol) in ethanol (20 mL) and the mixture was refluxed for an hour. The temperature was turned off to reach room temperature and the white solid was collected by filtration and dried to yield the title compound **3** (1,25 g, 38%). En: 289–292 °C. IR (KBr): υmax 3085, 2929, 1655, 1413, 1393, 1281, 770,764. ^1H NMR (500 MHz, DMSO) δ 12.24 (*s,* 1H, NH), 8.88 (*s,* 1H, Ar H), 8.62 (dd, *J* = 7.8, 1.1 Hz, 1H, Ar H), 8.34 (dd, *J* = 4.6, 1.3 Hz, 1H, Ar H), 8.07 (*d,* *J* = 1.8 Hz, 1H, Ar H), 7.25 (dd, *J* = 7.8, 4.7 Hz, 1H, Ar H). ^{13}C NMR (126 MHz, DMSO) δ 155.87 (Ar C), 150.01 (C=N), 144.55 (Ar C), 132.69 (Ar C), 130.66 (Ar C), 117.52 (Ar C), 111.23 (Ar C), 56.49 (Ar C), 19.03 (Ar C). **[**M+H]$^+$: calculated 289,1202; found: 289,1175.

*4.3. General procedure for the preparation of hydrazide linked 7-azaindoles (**5a–e**)*

Triethylamine (1 mmol) and acyl chloride (1 mmol) were added sequentially to the suspension of indole (1 mmol) in CH_3CN (20 mL) solvent and the mixture was rotated at room temperature for two hours. The solvent was evaporated without heating, the methyl acetyl hydrazines collected by filtration with the addition of water and dried. Column chromatography was also carried out to obtain products.

*4.4. (Z)-N′-{(1H-pyrrolo[2,3-b]pyridin-3-yl)methylene}acetohydrazide (**5a**)*

The acetohydrazide **5a** was prepared from hydrazonomethyl **4** (0.15 g, 0.94 mmol), triethylamine (0.13 mL, 1.00 mmol) and asetic anhydrite (0.09 mL, 1.00 mmol) according to GP-1 to give the title compound as white solid (0.18 g, 95%). IR (KBr): υmax 3085, 2929, 1655, 1413, 1393, 1281, 770, 764. ^1H NMR (500 MHz, DMSO) δ 11.16 (s, 1H, NH), 10.96 (s, 1H, NH), 8.43 – 8.38 (*m*, 1H, Ar H), 8.30-8.26 (*m,* 1H, Ar H), 8.14 (*s,* 2H, H2), 7.85 (*d,* *J* = 12.8 Hz, 1H, Ar H), 7.20 (dd, *J* = 7.7, 4.7 Hz, 1H, Ar H), 2.23 (*s,* 3H, Me). ^{13}C NMR (126 MHz, DMSO) δ 172.13 (C=O), 165.86 (Ar C), 149.62 (C=N), 144.41 (Ar C), 143.05 (Ar C), 140.24 (Ar C), 130.46 (Ar C), 117.42 (Ar C), 110.85 (Ar C), 20.80 (Me). **[**$M + H$]$^+$: calculated 203,0933; found: 203,0945.

*4.5. (Z)-N′-{(1H-pyrrolo[2,3-b]pyridin-3-yl)methylene}benzohydrazide (**5b**)*

The benzohydrazide **5b** was prepared from hydrazonomethyl **4** (0.4 g, 2.49 mmol), triethylamine (0.35 mL, 1.00 mmol) and benzoyl chloride (0.29 mL, 1.00 mmol) according to GP-1 to give the title compound as white solid (0.53 g, 80%). IR (KBr): υmax 3032, 2898, 1614, 1575, 1300, 1281, 1124, 770, 694. ^1H NMR (500 MHz, DMSO) δ 12.11 (*s,* 1H, NH), 11.63 (*s,* 1H, NH), 8.60 (*s,* 2H, Ar H), 8.32 (*d,* *J* = 3.5 Hz, 1H, H2), 7.92–7.98 (*m,* 3H, Ar H), 7.62-7.49 (*m,* 3H, Ar H), 7.24 (dd, *J* = 7.8, 4.8 Hz, 1H, Ar H). ^{13}C NMR (126 MHz, DMSO) δ 163.12 (C=O), 149.83(C=N), 144.87 (Ar C), 144.50 (Ar C), 134.41 (Ar C), 131.87 (Ar C), 130.91 (Ar C), 130.62 (Ar C), 129.72 (Ar C), 128.88 (Ar C), 127.96 (Ar C), 117.26 (Ar C), 117.18 (Ar C), 111.12 (Me). **[**$M + H$]$^+$: calculated 265,1089; found: 265,1125.

*4.6. (Z)-N′-{(1H-pyrrolo[2,3-b]pyridin-3-yl)methylene}-4-methylbenzohydrazide (**5c**)*

The benzohydrazide **5c** was prepared from hydrazonomethyl **4** (0.4 g, 2.49 mmol), triethylamine (0.49 mL, 1.00 mmol) and 4-methyl benzoyl chloride (0.46 mL, 1.00 mmol)) according to GP-1 to give the title compound as yellow solid (0.83 g, 85%). IR (KBr): υmax 3031, 2892, 1614, 1582, 1415, 1303, 1281, 1126, 770, 763. ^1H NMR (500 MHz, DMSO) δ 12.09 (*s,* 1H, NH), 11.55 (*s,* 1H, NH), 8.59 (*s,* 2H, Ar H), 8.32 (*s,* 1H, Ar H), 7.97 (*s,* 1H, Ar H), 7.84 (*d,* *J* = 7.3 Hz, 2H, Ar H), 7.32 (dd, *J* = 15.2, 7.7 Hz, 2H, Ar H), 7.23 (*d,* *J* = 4.9 Hz, 1H, H2), 2.39 (*s,* 3H, Me). ^{13}C NMR (126 MHz, DMSO) δ 162.95 (C=O), 155.88 (Ar C), 150.00 (C=N), 144.55 (Ar C), 141.84 (Ar C), 132.69 (Ar C), 131.49 (Ar C), 130.77 (Ar C), 130.68 (Ar C), 129.40 (Ar C), 127.98 (Ar C), 117.53 (Ar C), 117.25 (Ar C), 111.20 (Ar C), 21.48 (Me). **[**$M + H$]$^+$: calculated 279,1246; found: 279,1255.

*4.7. (Z)-N′-{(1H-pyrrolo[2,3-b]pyridin-3-yl)methylene}-4-nitrobenzohydrazide (**5d**)*

The benzohydrazide **5d** was prepared from hydrazonomethyl **4** (0.51 g, 3.18 mmol), triethylamine (0.44 mL, 1.00 mmol) and 4-nitro benzoyl chloride (0.59 g, 1.00 mmol) according to GP-1 to give the title compound as orange solid (0.79 g, 80%). IR (KBr): υmax 3160, 2929, 1646, 1522, 1416, 1330, 1280, 1125, 1105, 862, 772, 713. ^1H NMR (500 MHz, DMSO) δ 12.17 (*s,* 1H, NH), 11.94 (*s,* 1H, NH), 8.63 (*s,* 1H, H2), 8.59 (*d,* *J* = 7.7 Hz, 1H, Ar H), 8.38 (*d,* *J* = 8.6 Hz, 2H, Ar H), 8.33 (*d,* *J* = 3.1 Hz, 1H, Ar H), 8.17 (*d,* *J* = 8.6 Hz, 2H, Ar H), 8.03 (*s,* 1H, Ar H), 7.25 (dd, *J* = 7.7, 4.7 Hz, 1H, Ar H). ^{13}C NMR (126 MHz, DMSO) δ 161.41 (C=O), 149.86 (C=N), 149.56 (Ar C), 146.00 (Ar C), 144.58 (Ar C), 140.10 (Ar C), 131.50 (Ar C), 131.14 (Ar C), 130.59 (Ar C), 129.51 (Ar C), 124.08 (Ar C), 117.46 (Ar C), 117.15 (Ar C), 110.90 (Ar C). **[**$M + H$]$^+$: calculated 309,279; found: 309,453.

*4.8. (Z)-N′-{(1H-pyrrolo[2,3-b]pyridin-3-yl)methylene}-3-(trifluoromethyl)benzohydrazide (**5e**)*

The benzohydrazide **5e** was prepared from hydrazonomethyl **4** (0.3 g, 3.18 mmol), triethylamine (0.26 mL, 1.20 mmol) and 4-(triflоromethyl)benzoyl chloride (0.24 mL, 1.00 mmol) according to GP-1 to give the title compound as yellow solid (0.38 g, 61%). IR (KBr): υmax 3134, 3033, 2894, 1646, 1455, 1398, 1320, 1281, 1117, 793, 693. ^{1}H NMR (500 MHz, DMSO) δ 12.15 (*s,* 1H, NH), 11.84 (*s,* 1H, NH), 8.62 (*s,* 1H, CH), 8.34-8.32 (*m,* 1H, Ar H), 8.28-8.23 (*m,* 3H, Ar H), 8.02 (*s,* 1H, Ar H), 7.96 (*d, J* = 7.4 Hz, 1H, Ar H), 7.79 (*t, J* = 7.8 Hz, 1H, Ar H), 7.25 (dd, *J* = 7.8, 4.7 Hz, 1H, Ar H). ^{13}C NMR (126 MHz, DMSO) δ 161.61 (C=O), 155.87 (Ar C), 149.86 (C=N), 145.64 (Ar C), 144.56 (Ar C), 135.28 (Ar C), 132.16 (Ar C), 131.30 (Ar C), 130.58 (Ar C), 130.24 (Ar C), 128.45 (Ar C), 124.50 (CF_3), 117.42 (Ar C), 117.16 (Ar C), 110.95 (Ar C). **[***M* + *H*]$^+$: calculated 333,0963; found: 333,0947.

*4.9. (Z)-N′-{(1-benzoyl-1H-pyrrolo[2,3-b]pyridin-3-yl)methylene}benzohydrazide (**6b**)*

The benzohydrazide **6b** was prepared from hydrazonomethyl **4** (0.40 g, 1,00 mmol), triethylamine (0.55 mL, 1.50 mmol) and benzoyl chloride (0.45 mL, 1.50 mmol) according to GP-1 to give the title compound as white solid (0.18 g, 21%). IR (KBr): υmax 3330, 3048, 1665, 1550, 1402, 1265, 1175, 695, 681. ^{1}H NMR (500 MHz, DMSO) δ 12.00 (*s,* 1H, NH), 8.78 (*d, J* = 7.0 Hz, 1H, Ar H), 8.66 (*s,* 1H, Ar H), 8.44 (*s,* 1H, Ar H), 8.29 (*d, J* = 3.6 Hz, 1H, Ar H), 7.96 (*d, J* = 7.4 Hz, 2H, Ar H), 7.82 (*d, J* = 7.5 Hz, 2H, Ar H), 7.72 (*t, J* = 7.4 Hz, 1H, Ar H), 7.64-7.53 (*m,* 6H, Ar H), 7.44 (dd, *J* = 7.8, 4.8 Hz, 1H, Ar H). ^{13}C NMR (126 MHz, DMSO) δ 167.51 (C=O), 163.52 (C=N), 148.79 (Ar C), 145.52 (Ar C), 142.94 (Ar C), 133.99 (Ar C), 133.52 (Ar C), 132.19 (Ar C), 131.92 (Ar C), 131.19 (Ar C), 130.59 (Ar C), 128.95 (Ar C), 128.74 (Ar C), 128.12 (Ar C), 120.44 (Ar C), 120.17 (Ar C), 115.78 (Ar C). **[***M* + *H*]$^+$: calculated 369,1352; found: 369,1367.

*4.10. (Z)-4-methyl-N′-{(1-(4-methylbenzoyl)-1H-pyrrolo [2,3-b]pyridin-3-yl)methylene}benzohydrazide (**6c**)*

The benzohydrazide **6c** was prepared from hydrazonomethyl **4** (0.40 g, 1.00 mmol), triethylamine (0.53 mL, 1.50 mmol) and tosyl chloride (0.50 mL, 1.50 mmol) according to GP-1 to give the title compound as brown solid (0.18 g, 19%). IR (KBr): υmax 3206, 1678, 1651, 1399, 1268, 1167, 760, 745. ^{1}H NMR (500 MHz, DMSO) δ 11.91 (*s,* 1H, NH), 8.78 (*d, J* = 7.7 Hz, 1H, Ar H), 8.64 (*s,* 1H, Ar H), 8.41 (*s,* 1H, Ar H), 8.30 (*d, J* = 3.9 Hz, 1H, Ar H), 7.87 (*d, J* = 7.9 Hz, 2H, Ar H), 7.72 (*d, J* = 7.9 Hz, 2H, Ar H), 7.47-7.26 (*m,* 7H, Ar H), 2.42 (*s,* 3H, Me), 2.40 (s, 3H, Me). ^{13}C NMR (126 MHz, DMSO) δ 167.38 (C=O), 163.32 (C=N), 148.79 (Ar C), 145.48 (Ar C), 144.15 (Ar C), 142.70 (Ar C), 142.23 (Ar C), 131.89 (Ar C), 131.41 – 130.83 (Ar C), 129.79 (Ar C), 129.69 - 129.24 (Ar C), 128.13 (Ar C), 120.32 (Ar C), 120.07 (Ar C), 115.58 (Ar C), 21.76 (Me), 21.52 (Me). [*M* + *H*]$^+$: calculated 397,1665; found: 397,1702.

*4.11. General procedure for the preparation of 7-azaindole based 1,3,4-oxadiazoles (**7b-c, e**)*

I_2 (1.5 mmol) and K_2CO_3 (4.7 mmol) were added sequentially to the suspension of methyl acetyl hydrazines (1 mmol) in DMSO (3 mL) solvent, and the mixture was rotated at 110 °C for 48 h. After the reaction temperature was turned off and cooled, 5% Na_2SO_3 solution was added until the color turned white, 1,3,4 oxadiazoles were extracted with DCM and dried.

*4.12. 2-phenyl-5-(1H-pyrrolo[2,3-b]pyridin-3-yl)-1,3,4-oxadiazole (**7b**)*

Oxadiazole **7b** was prepared from benzohydrazide **5b** (0.34 g, 1,02 mmol), iodide (0.4 g, 1,58 mmol) and potassium carbonate (0.65 g, 4.70 mmol) according to GP-2 to give the title compound as yellow solid (0,12 g, 53%). IR (KBr): υmax 3088, 2924, 1577, 1414, 1277, 1024, 772, 726, 687. ^{1}H NMR (500 MHz, DMSO) δ 12.66 (*s,* 1H, NH), 8.51 (*d, J* = 7.9 Hz, 1H, Ar H), 8.47 (*s,* 1H, H2), 8.43-8.40 (*m,* 1H Ar H), 8.15 (dd, *J* = 6.5, 2.8 Hz, 2H, Ar H), 7.66-7.62 (*m,* 3H, Ar H), 7.34 (dd, *J* = 7.9, 4.7 Hz, 1H, Ar H). ^{13}C NMR (126 MHz, DMSO) δ 162.38 (Ar C), 161.52 (Ar C), 148.92 (Ar C), 144.74 (Ar C), 131.93 (Ar C), 129.63 (Ar C), 129.21 (Ar C), 128.93 (Ar C), 126.68 (Ar C), 123.79 (Ar C), 116.75 (Ar C), 98.55 (Ar C). **[***M* + *H*]$^+$: calculated 263,0933; found: 263,0920.

*4.13. 2-(1H-pyrrolo[2,3-b]pyridin-3-yl)-5-(p-tolyl)-1,3,4-oxadiazole (**7c**)*

Oxadiazole **7c** was prepared from benzohydrazide **5c** (0.34 g, 1,02 mmol), iodide (0.4 g, 1,58 mmol) and potassium carbonate (0.65 g, 4.70 mmol) according to GP-2 to give the title compound as yellow solid (0,1 g, 51%). IR (KBr): υmax 3082, 2852, 1576, 1497, 1411, 1278, 1018, 820, 793, 771, 732. ^{1}H NMR (500 MHz, DMSO) δ 12.64 (*s,* 1H, NH), 8.50 (*d, J* = 7.7 Hz, 1H, Ar H), 8.45 (*d, J* = 2.5 Hz, 1H, H2), 8.41 (*d, J* = 4.5 Hz, 1H, Ar H), 8.03 (*d, J* = 8.0 Hz, 2H, Ar H), 7.45 (*d, J* = 8.0 Hz, 2H, Ar H), 7.34 (dd, *J* = 7.9, 4.7 Hz, 1H, Ar H), 2.42 (*s,* 3H, Me). ^{13}C NMR (126 MHz, DMSO) δ 162.70 (Ar C), 161.52 (Ar C), 149.19 (Ar C), 144.96 (s), 142.26 (Ar C), 130.41 (Ar C), 129.34 (Ar C), 129.17 (Ar C), 126.89 (Ar C), 121.33 (Ar C), 118.06 (Ar C), 117.00 (Ar C), 98.87 (Ar C), 21.62 (Me). **[***M* + *H*]$^+$: calculated 277,1089; found: 277,1042.

2-(1H-pyrrolo[2,3-b]pyridin-3-yl)-5-(3-(trifluoromethyl)phenyl)-1,3,4-oxadiazole (7e) Oxadiazole **7e** was prepared from benzohydrazide **5e** (0.34 g, 1,02 mmol), iodide (0.4 g, 1,58 mmol) and potassium carbonate (0.65 g, 4.70 mmol) according to GP-2 to give the title compound as yellow solid (0,2 g, 48%). IR (KBr): υmax 3095, 2920, 2850, 1575, 1324, 1176, 1120, 899, 770, 692. ^{1}H NMR (500 MHz, DMSO) δ 12.71 (*s,* 1H, NH), 8.56 (*s,* 1H, Ar H), 8.52 (dd, *J* = 7.9, 1.5 Hz, 1H, Ar H), 8.47 (*d, J* = 12.3 Hz, 1H, Ar H), 8.45-8.43 (*m,* 1H, Ar H), 8.40 (*s,* 1H, H2), 8.02 (*d, J* = 7.8 Hz, 1H, Ar H), 7.90 (*t, J* = 7.8 Hz, 1H, Ar H), 7.36 (dd, *J* = 7.9, 4.7 Hz, 1H, Ar H). ^{13}C NMR (126 MHz, DMSO) δ 185.85 (Ar C), 174.24 (Ar C), 162.18 (Ar C), 161.50 (Ar C), 149.18 (Ar C), 144.97 (Ar C), 131.20 (Ar C), 130.80 (Ar C), 129.94 (Ar C), 129.13 (Ar C), 128.51 (*d, J* = 3.5 Hz, CF_3), 125.13 (Ar C), 118.84 (Ar C), 118.10 (Ar C), 116.95 (Ar C), 98.58 (Ar C). **[***M* + *H*]$^+$: calculated 331,0807; found: 331,0797.

4.14. α-glucosidase inhibitory assay

The α-glucosidase inhibition activity was performed according to method given by Taha et al. [37]. The reaction mixture contained 70 μL of 50 mM phosphate buffer (pH 6.8), 10 μL (0.5 mM in methanol) of the test compound, and an additional 10 μL (0.057 unit, Sigma Inc.) of the α-glucosidase solution in the buffer. After mixing all the contents, reaction mixture was incubated for 10 min at 37 °C and preread at 400 nm. The reaction was initiated by the addition of 10 μL of 0.5 mM substrate (p-nitrophenyl glucopyranoside, Sigma Inc.). Following 30 min of incubation at 37 °C, the absorbance of p-nitrophenol was measured at 400 nm using the 96-well plate reader (Thermo Scientific). Acarbose was used as positive control. All assays were performed in triplicate (mean ± SEM, *n* = 3). Percent inhibition was calculated by the following equation:

Inhibition(%) = ((Absorbance of control- Absorbance of test)/ Absorbance of control))

IC_{50} concentrations were calculated using concentration vs. percent inhibition values.

4.15. Antioxidant assays

4.15.1. 2,2-diphenyl-2-picryl-hydrazyl (DPPH) assay

The DPPH antioxidant activity assay was performed by the method given by Gu et al. with slight modifications [38]. Briefly, 0.1 mM DPPH solution was prepared in methanol. The reaction mixture contained 260 µL of the DPPH solution and 40 µL of test compound. The mixture was incubated for 30 min at room temperature. Then the absorbance was measured at 517 nm using the 96-well plate reader (Thermo Scientific). All assays were performed in triplicate (mean ± SEM, $n = 3$). Percent inhibition was calculated by the following equation:

Inhibition(%) = ((Absorbance of control- Absorbance of test)/ Absorbance of control))

IC50 concentrations were calculated using concentration vs. percent inhibition values.

4.16. 2,2′-azino-bis(3-ethylbenzthiazoline-6-sulfonic acid) (ABTS) assay

The ABTS antioxidant activity assay was performed by the method given by Gu et al. with slight modifications [38]. Briefly, 5 mL of 7 mM ABTS solution and 88 μL of 140 mM potassium persulfate solution were mixed and incubated at room temperature for 16 h at dark. Following the incubation, 0.5 mL of the reaction mixture was diluted with 45 mL of ethanol and the absorbance was adjusted to 0.7. Later, 10 μL of test compound (1000, 500, 250, 125, 62.5, 31.25, 15.60, 7.80 μg/mL) and 290 μL of reaction mixture were mixed. The absorbance was measured at 734 nm using the 96-well plate reader (Thermo Scientific) after 6 min incubation. All assays were performed in triplicate (mean ± SEM, $n = 3$). Percent inhibition was calculated by the following equation:

Inhibition(%) = ((Absorbance of control- Absorbance of test)/ Absorbance of control))

IC50 concentrations were calculated using concentration vs. percent inhibition values.

4.17. Computational methods

In order to get insights into the plausible binding mode of synthesis compounds to the target protein, Lysosomal alpha-glucosidase (GAA), Glide by Schrodinger Inc. and AutoDock vina [39] docking software were used with previously reported protocols [40–44]. Crystallography studies of GAA-inhibitor complexes showed that glycans can attach to the protein from various positions on the surface. However, alpha-acarbose was co-crystallized with GAA in two distinct positions one of which is the active side. Thus, we have used these locations as the docking grids.

4.18. Protein preparation

Lysosomal alpha-glucosidase (GAA) protein complexed with alpha-acarbose (AC1) and acorbose-derived trisaccharide inhibitors (PDB id= 5NN8 and 5KZW) was used in computational studies. Preliminary to docking, homology modeling was carried out using SWISS-MODEL [45]. The template sequence named 5 kzw.1.A provided 99.7% similarity. Protein-ligand complex was preprocessed to add hydrogens, assign bond orders and remove other contaminants using the Schrodinger Suite. The pKa of each residue at pH=6.8 was calculated using the PROPKA tool included in the protein preparation wizard module in the suite. The minimization process was performed using the OPLS_2005 force field by constraining heavy atoms to 0.30 Å deviation. Corresponding pdbqt file for AutoDock vina was generated.

4.19. Ligand preparation

The sdf files with 3D structures of 11 synthesized molecules were generated with Gaussview 6 [46]. LigPrep module in Schrodinger Suite was used to generate all possible conformers with OPLS_2005 force field and pH=6.8. Ligands built for AutoDock vina were converted to pdbqt format with OpenBabel tool [47].

4.20. Grid generation

In Glide, the Receptor Grid Generation module was used to generate two different grids for both alpha-acarbose (AC1) and acarbose derived trisaccharide (AC2) inhibitors. Due to the large size of AC1 and AC2 ligands, $20 \times 20 \times 20$ Å^3 grid box was generated for both regions. In vina, the same grids were generated.

4.21. Docking protocol

Default parameters in Glide Ligand Docking module were used. The precision was adjusted to Extra Precision (XP) for producing a maximum of 40 poses. The ligand and protein were described as a flexible. Default parameters in vina was used except exhaustiveness 20 was selected and produced 20 poses.

Declaration of Competing Interest

There is no declaration of interest.

CRediT authorship contribution statement

Samet Izgi: Investigation. **Ibrahim F. Sengul:** Conceptualization, Writing – review & editing, Writing – original draft. **Engin Şahin:** Validation. **Mehmet Serdar Koca:** Formal analysis, Software, Writing – original draft. **Fatma Cebeci:** Investigation, Writing – original draft. **Hakan Kandemir:** Conceptualization, Writing – original draft, Writing – review & editing.

Acknowledgments

This work has been supported by The Scientific and Technological Research Council of Turkey (Project Number: 120Z116) and Tekirdag Namık Kemal University (Project Number: NKUBAP.01.GA.19.220).

Supplementary materials

Supplementary material associated with this article can be found, in the online version, at doi:10.1016/j.molstruc.2021.131343.

References

[1] N. Kerru, L. Gummidi, S. Maddila, K.K. Gangu, S.B. Jonnalagadda, A review on recent advances in nitrogen-containing molecules and their biological applications, Molecules 25 (1909) 2020.
[2] M.M. Heravi, V. Zadsirjan, Prescribed drugs containing nitrogen heterocycles: an overview, RSC Adv. 10 (2020) 44247.
[3] I.F. Sengul, K. Wood, N. Kumar, D. StC Black, Synthesis of macrocyclic systems derived from di-(2-indolyl) heteroarenes, Tetrahedron 68 (2012) 9050.
[4] I.F. Sengul, E. Astarci, H. Kandemir, Synthesis of Novel Pyrrolo [3, 2-c] carbazole and Dipyrrolo [3, 2-c: 2′, 3′-g] carbazole Derivatives, Synlett 27 (2016) 1277.
[5] P.S Shaveta, Structural optimization of indole based compounds for highly promising anti-cancer activities: Structure activity relationship studies and identification of lead molecules, Eur. J. Med. Chem. 74 (2014) 440.
[6] S.K. Sharma, P. Kumar, B. Narasimhan, K. Ramasamy, V. Mani, R.K. Mishra, A.B. Majeed, Synthesis, antimicrobial, anticancer evaluation and QSAR studies of 6-methyl-4-[1-(2-substituted-phenylamino-acetyl)-1H-indol-3-yl]-2-oxo/thioxo-1,2,3,4-tetrahydropyrimidine-5-carboxylic acid ethyl esters, Eur. J. Med. Chem. 48 (2012) 16.
[7] N.K. Kaushik, N. Kaushik, P. Attri, N. Kumar, C.H. Kim, A.K. Verma, E.H. Choi, Biomedical importance of indoles, Molecules 18 (2013) 6620.

[8] S. Ayari, M.F. Sağlam, E. Şenkuytu, P.B. Erçin, Y. Zorlu, I.F. Sengul, B. Jamoussi, D. Atilla, 3-Methylindole-substituted zinc phthalocyanines for photodynamic cancer therapy, J. Porphyr. Phthalocyanines 23 (2019) 1371.
[9] M.F. Saglam, M. Bingul, E. Şenkuytu, M. Boga, Y. Zorlu, H. Kandemir, I.F. Sengul, Synthesis, characterization, UV–Vis absorption and cholinesterase inhibition properties of bis-indolyl imine ligand systems, J. Mol. Struct. 1215 (2020) 128308.
[10] Y.S. Tung, M.S. Coumar, Y.S. Wu, H.Y. Shiao, J.Y. Chang, J.P. Liou, P. Shukla, C.W. Chang, C.Y. Chang, C.C. Kuo, T.K. Yeh, C.Y. Lin, J.S. Wu, S.Y. Wu, C.C. Liao, H.P. Hsieh, Scaffold-hopping strategy: synthesis and biological evaluation of 5, 6-fused bicyclic heteroaromatics to identify orally bioavailable anticancer agents, J. Med. Chem. 54 (2011) 3076.
[11] D.R. Motati, R. Amaradhi, T. Ganesh, Recent developments in the synthesis of azaindoles from pyridine and pyrrole building blocks, Org. Chem. Front. 8 (2021) 466.
[12] M.J.D. Pires, D.L. Poeira, S.I. Purificação, M.M.B. Marques, Synthesis of substituted 4-, 5-, 6-, and 7-azaindoles from aminopyridines via a cascade C–N cross-coupling/heck reaction, Org. Lett. 18 (2016) 3250.
[13] S.B. Zhao, S. Wang, Luminescence and reactivity of 7-azaindole derivatives and complexes, Chem. Soc. Rev. 39 (2010) 3124.
[14] J.Y. Mérour, F. Buron, K. Plé, P. Bonnet, S. Routier, The azaindole framework in the design of kinase inhibitors, Molecules 19 (2014) 19935.
[15] U.K. Bandarage, J. Cao, J.H. Come, J.J. Court, H. Gao, M.D. Jacobs, C. Marhefka, S. Nanthakumar, J. Green, ROCK inhibitors 3: Design, synthesis and structure-activity relationships of 7-azaindole-based Rho kinase (ROCK) inhibitors, Bioorg. Med. Chem. Lett. 28 (2018) 2622.
[16] R. Cincinelli, L. Musso, L. Merlini, G. Giannini, L. Vesci, F.M. Milazzo, N. Carenini, P. Perego, S. Penco, R. Artali, F. Zunino, C. Pisano, S. Dallavalle, 7-Azaindole-1-carboxamides as a new class of PARP-1 inhibitors, Bioorg. Med. Chem. 22 (2014) 1089.
[17] G. Trimurtulu, D.J. Faulkner, N.B. Perry, L. Ettouati, M. Litaudon, J.W. Blunt, M.H.G. Munro, G.B. Jameson, Alkaloids from the antarctic sponge Kirkpatrickia varialosa. Part 2: Variolin A and N (3′)-methyl tetrahydrovariolin B, Tetrahedron 50 (1994) 3993.
[18] P.E. Harrington, M.P. Bourbeau, C. Fotsch, M. Frohn, A.J. Pickrell, A. Reichelt, K. Sham, A.C. Siegmund, J.M. Bailis, T. Bush, S. Escobar, D. Hickman, S. Heller, F. Hsieh, J.N. Orf, M. Rong, T.S. Miguel, H. Tan, L. Zalameda, J.G. Allen, The optimization of aminooxadiazoles as orally active inhibitors of Cdc7, Bioorg. Med. Chem. Lett. 23 (2013) 6369.
[19] G. Kesan, B. Topaloglu, E. Ozcan, H.H. Kazan, E.T. Ecik, E. Şenkuytu, I.F. Sengul, H. Kandemir, B. Cosut, Azaindole-BODIPYs: Synthesis, fluorescent recognition of hydrogen sulfate anion and biological evaluation, Spectrochim. Acta A 213 (2019) 73.
[20] Y.Z. Dai, N.A.Y. Lu, Y.Q. Zheng, J.H. Dou, K. Shi, T. Lei, J.Y. Wang, J. Pei., Embedding electron-deficient nitrogen atoms in polymer backbone towards high performance n-type polymer field-effect transistors, Chem. Sci. 7 (2016) 5753.
[21] S.B. Zhao, S. Wang, Luminescence and reactivity of 7-azaindole derivatives and complexes, Chem. Soc. Rev. 39 (2010) 3142.
[22] S. Narva, S. Chitti, B.R. Bala, M. Alvala, N. Jain, V.G.C.S. Kondapalli, Synthesis and biological evaluation of pyrrolo[2,3-b]pyridine analogues as antiproliferative agents and their interaction with calf thymus DNA, Eur. J. Med. Chem. 114 (2016) 220.
[23] J. Boström, A. Hogner, A. Llinàs, E. Wellner, A.T. Plowright, Oxadiazoles in medicinal chemistry, J. Med. Chem. 55 (2011) 1817.
[24] A. Vaidya, D. Pathak, K. Shah, 1, 3, 4-oxadiazole and its derivatives: A review on recent progress in anticancer activities, Chem. Biol. Drug Des. 97 (2021) 572.
[25] Z. Li, P. Zhan, X. Liu, 1, 3, 4-Oxadiazole: A privileged structure in antiviral agents, Mini Rev. Med. Chem. 11 (2011) 1130.
[26] S.L. Gaonkar, K.M. Rai, B. Prabhuswamy, Synthesis and antimicrobial studies of a new series of 2-{4-[2-(5-ethylpyridin-2-yl)ethoxy]phenyl}-5-substituted-1,3,4-oxadiazoles, Eur. J. Med. Chem. 41 (2006) 841.
[27] A.A. El-Emam, O.A. Al-Deeb, M. Al-Omar, J. Lehmann, Synthesis, antimicrobial, and anti-HIV-1 activity of certain 5-(1-adamantyl)-2-substituted thio-1,3,4-oxadiazoles and 5-(1-adamantyl)-3-substituted aminomethyl-1,3,4-oxadiazoline-2-thiones, Bioorg. Med. Chem. 12 (2004) 5107.
[28] F.A. Omar, N.M. Mahfouz, M.A. Rahman, Design, synthesis and antiinflammatory activity of some 1, 3, 4-oxadiazole derivatives, Eur. J. Med. Chem. 31 (1996) 819.
[29] J. Chiang, G. Hermodsson, S. Oie, The Effect of α_1-acid glycoprotein on the pharmacological activity of α_1-adrenergic antagonists in rabbit aortic strips, J. Pharm. Pharmacol. 43 (1991) 540.
[30] M. Bingul, M.F. Saglam, H. Kandemir, M. Boga, I.F. Sengul, Synthesis of indole-2-carbohydrazides and 2-(indol-2-yl)-1, 3, 4-oxadiazoles as antioxidants and their acetylcholinesterase inhibition properties, Monatshefte Chem. 150 (2019) 1553.
[31] Y.S. Li, M. He, T.S. Zhou, Q. Wang, L. He, S.J. Wang, B. Hu, B. Wei, H. Wang, Z.N. Cui, 2, 5-Disubstituted furan derivatives containing 1, 3, 4-thiadiazole moiety as potent α-glucosidase and E. coli β-glucuronidase inhibitors, Eur. J. Med. Chem. 216 (2021) 113322.
[32] N. Mihailovic, V. Markovic, I.Z. Matic, N.S. Stanisavljevic, Z.S. Jovanovic, S. Trifunovic, L. Joksovic, Synthesis and antioxidant activity of 1, 3, 4-oxadiazoles and their diacylhydrazine precursors derived from phenolic acids, RSC Adv. 7 (2017) 8550.
[33] K. Kaur, S. Chaudhary, S. Singh, S.K. Mehta, An azaindole–hydrazine imine moiety as sensitive dual cation chemosensor depending on surface plasmon resonance and emission properties, Sens. Actuators B 222 (2016) 397.
[34] L. Ma, Y. Xiao, C. Li, Z.L. Xi, D.D. Li, Y.T. Wang, H.T. Ma, H.L. Zhu, M.H. Wang, Y.H. Ye, Synthesis and antioxidant activity of novel Mannich base of 1,3,4-oxadiazole derivatives possessing 1,4-benzodioxan, Bioorg. Med. Chem. 21 (2013) 6763.
[35] H. Panwar, D. Calderwood, I.R. Grant, S. Grover, B.D. Green, Lactobacillus strains isolated from infant faeces possess potentinhibitory activity against intestinal alpha- and beta-glucosidasessuggesting anti-diabetic potential, Eur. J. Nutr. 53 (2014) 1465.
[36] Y. Kyriachenko, T. Falalyeyeva, O. Korotkyi, N. Molochek, N. Kobyliak., Crosstalk between gut microbiota and antidiabetic drug action, World J. Diabetes 10 (2019) 154.
[37] M. Taha, N.H. Ismail, S. Imran, A. Wodood, F. Rahim, M. Ali, A.U. Rehman, Novel quinoline derivatives as potent in vitro α-glucosidase inhibitors: in silico studies and SAR predictions, Med. Chem. Commun. 6 (2015) 1826.
[38] C. Gu, K. Howell, F.R. Dunshea, H.A.R. Suleria, LC-ESI-QTOF/MS characterisation of phenolic acids and flavonoids in polyphenol-rich fruits and vegetables and their potential antioxidant activities, Antioxidants 8 (2019) 405.
[39] O. Trott, A.J. Arthur, AutoDock Vina: Improving the speed and accuracy of docking with a new scoring function, efficient optimization, and multithreading, J. Comput. Chem. 31 (2010) 455.
[40] E. Bağda, E. Bağda, A. Kocak, M. Durmuş, Investigation of binding behaviour of a water-soluble gallium (III) phthalocyanine with double-stranded and G-quadruplex DNA via experimental and computational methods, J. Mol. Struct. 1240 (2021) 130536.
[41] S.Y. Al-Raqa, K. Khezami, E.N. Kaya, A. Kocak, M. Durmuş, Experimental and theoretical investigation of water-soluble silicon(IV) phthalocyanine and its interaction with bovine serum albumin, JBIC J. Biol. Inorg. Chem. 26 (2021) 235.
[42] A. Kocak, HBGA binding modes and selectivity in noroviruses upon mutation: A docking and molecular dynamics study, J. Mol. Model. 25 (2019) 369.
[43] A. Kocak, M. Yildiz, Docking, molecular dynamics and free energy studies on aspartoacylase mutations involved in Canavan disease, J. Mol. Graph. Model. 74 (2017) 44.
[44] A. Kocak, I. Erol, M. Yıldız, H. Can, Computational insights into the protonation states of catalytic dyad in BACE1–acyl guanidine based inhibitor complex, J. Mol. Graph. Model. 20 (2016) 226.
[45] L. Bordoli, F. Kiefer, K. Arnold, P. Benkert, J. Battey, T. Schwede, Protein structure homology modeling using SWISS-MODEL workspace, Nat. Protoc. 4 (1) (2009).
[46] M.J. Frisch, J. Michael "Gaussian09." http://www.gaussian.com/ (2009)
[47] N.M. O'Boyle, M. Banck, C.A. James, C. Morley, T. Vandermeersch, G.R. Hutchison, Open Babel: An open chemical toolbox, J. Cheminform. 3 (2011) 33.